Er-doped silicon nanowires with 1.54 m light-emitting and enhanced electrical and field emission properties

C. T. Huang, C. L. Hsin, K. W. Huang, C. Y. Lee, P. H. Yeh, U. S. Chen, and L. J. Chen

Citation: Applied Physics Letters **91**, 093133 (2007); doi: 10.1063/1.2777181
View online: http://dx.doi.org/10.1063/1.2777181
View Table of Contents: http://scitation.aip.org/content/aip/journal/apl/91/9?ver=pdfcov
Published by the AIP Publishing

Er-doped silicon nanowires with 1.54 μm light-emitting and enhanced electrical and field emission properties

C. T. Huang, C. L. Hsin, K. W. Huang, C. Y. Lee, P. H. Yeh, U. S. Chen, and L. J. Chen[a)]
Department of Material Science and Engineering, National Tsing Hua University, Hsinchu 300, Taiwan, Republic of China

(Received 21 May 2007; accepted 8 August 2007; published online 31 August 2007)

Erbium-doped silicon nanowires have been grown via a vapor transport and condensation method with $ErCl_3 \cdot 6H_2O$ powder as part of the source in one step. The Er-doped silicon nanowires exhibit the room temperature photoluminescence at a wavelength of 1.54 μm, ideal for optical communication. From *I-V* measurements, the resistivity of 4.2 at. % Er-doped Si nanowires was determined to be 1.5×10^{-2} Ω cm. The Er-doped silicon nanowires were found to possess excellent field emission properties with a field enhancement factor as high as 1260. The rich variety of enhanced physical properties exhibited by the Er-doped silicon nanowires points to versatile applications for advanced devices. © *2007 American Institute of Physics*. [DOI: 10.1063/1.2777181]

The incorporation of impurity centers in a given material has led to many advanced applications. Rare-earth element doped materials have been shown to be highly versatile in diverse applications, especially for optoelectronic devices. Since the early report in 1983,[1] the optical properties of erbium doped materials have been extensively investigated. The incorporation of Er^{3+} into semiconductors is a promising method to combine electronic devices with optical function. The intra-4*f*-shell transitions from Er^{3+} would exhibit a luminescence at the wavelength of 1.54 μm which is a crucial wavelength for transmission in silica-based optical fibers. The room-temperature operation of Er-doped silicon *p-n* diodes was demonstrated in 1994.[2] Erbium could be doped into different forms of structures which range from zero dimensional nanocrystals,[3] one dimensional nanowires (NWs) and nanotubes,[4–8] two dimensional thin film[9,10] to silicon wafers.[11]

In the past decade, silicon NWs have attracted a great deal of attention since silicon is the most vital semiconductor material. Silicon NWs are promising for applications in future nanoscale devices and as vehicles to explore the intriguing physical phenomena in nanoscale structures.[12–14] For optoelectronic applications, Er-doped silicon NWs have great potential because of its $^4I_{13/2} \rightarrow {}^4I_{15/2}$ luminescent transition near 1.54 μm used for telecommunication. The electrical properties of B- and P-doped silicon NWs were found to vary with doping species and concentration.[15,16] Doping erbium into silicon nanowires shall affect both the electrical and optical properties of silicon NWs.

Silicon (100) substrates were ultrasonically cleaned in acetone prior to the deposition of 2-nm-thick Au film by electron-beam evaporation. Er-doped silicon NWs were synthesized via a vapor transport and condensation process with the use of Au catalysts. The quartz tube inside the three-zone furnace was evacuated to a pressure below 10^{-5} torr using a diffusion pump. A constant flow of 60 SCCM (SCCM denotes cubic centimeter per minute at STP) Ar and 15 SCCM H_2 was introduced as a carrier gas through mass flow controllers and pumped through the quartz tube. The pressure inside the quartz tube was kept constant at 1 torr with a hand controlled valve. The three zones were heated from room temperature to reach 1100, 900, and 700 °C, respectively, at the same time. The silicon source in an alumina boat was placed upstream in the 1100 °C zone. The $ErCl_3 \cdot 6H_2O$ source in another alumina boat was positioned upstream and close to the Au-coated Si substrates in an alumina boat. Au-coated Si substrates were heated downstream in the middle of the 900 and 700 °C zones. After keeping the samples at the desired temperature for 90 min, the furnace was allowed to cool down to room temperature.

The surface morphology of the NWs was examined with a field-emission scanning electron microscope (FESEM) (JEOL JSM-6500F), operated at 15 kV. The transmission electron microscope (TEM) samples were scraped ultrasonically in ethanol and then dispersed on a Cu grid covered with a holey carbon film. A TEM (JEOL JEM-2010) equipped with an energy dispersive spectrometer (EDS) was used to determine the microstructures and chemical compositions. The *I-V* measurements were carried out in a multiprobe nanoelectronics measurement (MPNEM) system. The MPNEM system is composed of FESEM (JEOL JSM-7000F), nanomanipulator system with four tungsten probes (300 nm in tip size, Kammrath & Wiess GmbH), and *I-V* measurement system (Keithley model 4200-SCS). During the *I-V* measurement in the SEM, the electron beam was turn off to exclude the influence from the electron beam.

Figure 1 shows a top-view SEM image of the as-synthesized NWs after 90 min growth. The diameters of NWs were measured to range from 20 to 200 nm. The inset shows a side-view SEM image of the nanowires. The lengths of the nanowires are about 2–5 μm.

Figure 2 shows the TEM image of a 20 nm nanowire sheathed with a 1.5-nm-thick oxide layer. Analysis of the electron diffraction patterns indicate that the nanowires are single-crystal silicon with [110] growth direction, which has been observed for Si NWs grown by either vapor-liquid-solid or oxide-assisted mechanism.[17–20] From the EDS spectrum displayed in the inset, the silicon NW was found to consist of about 4.2 at. % erbium. The Cu and C signals originate from the Cu grid covered with C film.

[a)]Electronic mail: ljchen@mx.nthu.edu.tw

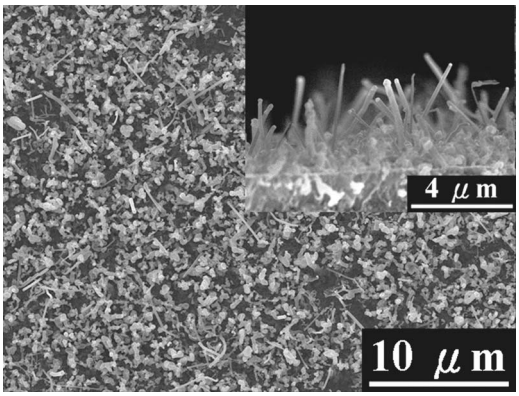

FIG. 1. Top-view SEM image of Er-doped silicon NWs. The inset shows the side-view SEM image.

Figure 3 shows the room-temperature photoluminescence (PL) spectrum of the Er-doped silicon NWs. The PL spectrum was pumped with a 514 nm Ar laser. The Er-doped silicon NWs display the characteristic Er^{3+} luminescence at the wavelength of 1.54 μm. The PL at 1.54 μm comes from the intra-4*f*-shell transitions of Er^{3+} doped in the silicon NWs. As a result, the silicon NWs are endowed with a significant optical function at room temperature through Er doping. On the other hand, for oxygen- and hydrogen-terminated silicon nanowires, Dovrat *et al.*[21] have found that the red- and the blue-emission bands from these nanowires are characterized by homogeneous broadening and are due to interface states in the silicon core and oxygen-based defects at the oxide cladding layer, respectively. It is expected that visible PL should be affected by the presence of Er, particularly since there are reports on resonant energy transfer, assisted by the silicon nanocrystals or nanowires to enhance the PL associated with Er. The influence of Er doping on SiNWs with controlled size in visible spectrum is an important subject that needs to be investigated.

The use of silicon in electronic devices is strongly dependent on the presence, species, and concentration of doping impurities able to control the Fermi level close to the conduction or valence band edges. The resistivity of silicon NWs would be reduced via the doping of impurities to increase carrier concentration. For *I-V* measurements, focused

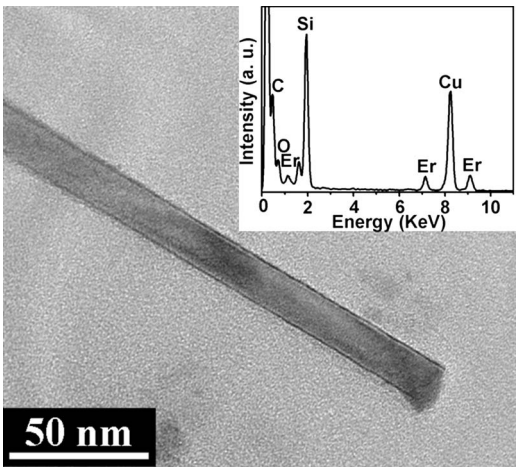

FIG. 2. Bright-field TEM image of an as-synthesized Er-doped silicon NW. Inset shows the corresponding EDS spectrum. The Cu and C signals come from the Cu grid covered with C film.

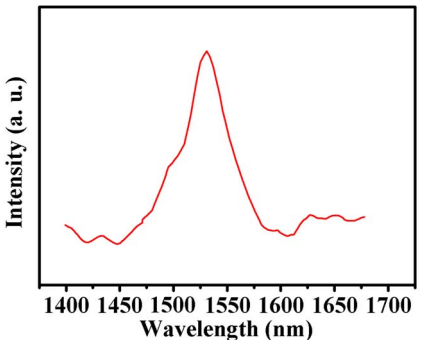

FIG. 3. (Color online) Room-temperature PL spectrum of Er-doped silicon NWs pumped with a 514 nm Ar laser.

ion-beam system was used to deposit square-shaped platinum layer as contacts at the two edges of Er-doped silicon NWs dispersed on the SiO_x/Si substrate, as shown in SEM image in the inset of Fig. 4. The Ohmic nature of the contact is indicated from the linear *I-V* relationship shown in Fig. 4. For impurity concentrations lower than the solid solubility, the contact resistivity between the contact metal and Er-doped SiNW is proportional to $\exp(\psi/N^{1/2})$, where ψ is the potential barrier between the contact metal and Er-doped Si NW and N is the impurity concentration in the Si NWs.[22] When the impurity concentration increases, the contact resistivity would decrease. The electrons would easily tunnel through the barrier between the contact metal and Er-doped Si NW. The resistance and resistivity of the 190 nm in diameter Er-doped silicon NW were calculated to be 3.49 k Ω and 1.5×10^{-2} Ω cm, respectively. The ressitvity is considerably lower than those of pure silicon (1×10^{4} Ω cm) and as-received silicon wafers (1–10 Ω cm). A detailed investigation of electrical and defect properties of Er-ion implanted Si showed that erbium doping introduced donor states.[23] The result indicates that Er atoms reside at the Si lattice sites and contribute to the electrical carriers to enhance the conductivity of the Si nanowires.

Figure 5 shows the current density (J) as a function of the applied electric field (E) with a separation of 220 μm between the anode and emitting surface. The turn-on field, defined as applied field for receiving current density of 1 μA cm^{-2}, was measured to be about 4.6 V μm^{-1}. The Fowler-Nordheim (FN) plot of $\ln(J/E^2)$ against $1/E$ is shown in the inset of Fig. 5. The FN plot indicates that the field-emission behavior obeys the FN rule for which the electrons can tunnel through the potential barrier from conduction band to vacuum state. The FN relationship can

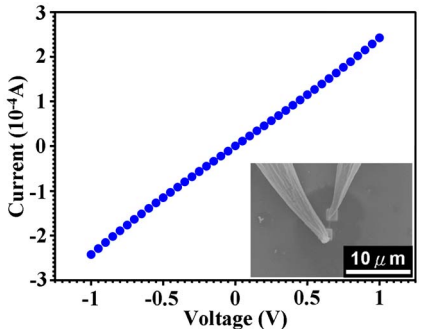

FIG. 4. (Color online) *I-V* curve of Er-doped silicon NWs. Inset shows the SEM image of the sample for *I-V* measurement.

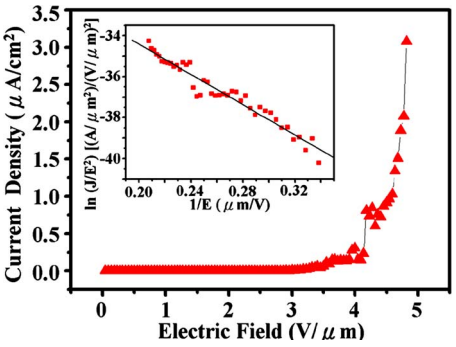

FIG. 5. (Color online) Field-emission curve of Er-doped silicon NWs as a function of applied electric field. Inset shows the corresponding $\ln(J/E^2)$-$1/E$ plot.

be expressed by a simplified equation. $J=(A\beta^2E^2/\varphi)\exp(-B\varphi^{3/2}/\beta E)$, where J is the current density, E is the applied field strength, φ is the work function. A and B are constants corresponding to 1.56×10^{-10} A eV/V^2 and 6.83×10^3 V/eV$^{3/2}$ μm, respectively. The field enhancement factor β was calculated to be 1260, based on a work function value of 3.6 eV. The β value compares favorably with that of tapered Si nanowires (1000) without any doping measured by Chueh *et al.*[24] The turn-on field of 4.6 V μm^{-1} is low compared to 6 V μm^{-1} for boron-doped Si particle chains.[25] The increase in the β value is attributed to the enhanced conductivity with doping impurities in silicon. The doping of erbium would elevate the carrier concentration and reduce the resistivity of silicon nanowires.

Silicon NWs have been considered to be the key part of the most promising technology to extend the size limit of the silicon-based electronic devices. Er surface-enriched silicon NWs were prepared by the pyrolysis of silane and a volatile erbium complex on a Au catalyst surface.[5] Optical activation of silicon NWs using sol-gel derived Er-doped silica has been demostrated.[6] In the present work, uniform Er-doping in the silicon NWs was achieved by a facile vapor transport and condensation method in one step. The doping results in light emission at 1.54 μm and a lowering of electrical resistivity. In addition, the NWs may also be used as field emitters with their excellent field emission properties. For practical applications, the variation in electrical, optical, and field emission properties with doping level as well as complex-forming species needs to be further investigated.[9,11,22] One can envision Er-doped silicon NWs serving as active components of field effect transistors as well as light emitters, detectors, and/or waveguides for optical applications, perhaps simultaneously. A recent work demonstrated the room temperature ferromagnetism for the Mn^+-implanted Si NWs, which may lead to spintronics application.[26] The rich variety of physical properties exhibited by the doped Si NWs points to versatile applications for advanced devices.

In summary, erbium-doped silicon NWs have been synthesized with a vapor transport and condensation method with $ErCl_3\cdot6H_2O$ powder as part of the evaporation source. The incorporation of erbium into the silicon NWs was verified by the TEM/EDS, *I-V* measurement, and PL. The Er-doped silicon NWs exhibit the room temperature PL spectrum at the wavelength of 1.54 μm which comes from the intra-4*f*-shell transitions of Er^{3+} doped in the silicon NWs. From *I-V* measurements, the resistivity of Er-doped silicon NWs was determined to be 1.5×10^{-2} Ω cm. The Er-doped silicon NWs were found to possess excellent field emission properties with a field enhancement factor as high as 1260.

The research was supported by the ROC National Science Council through Grant Nos. NSC 95-2221-E-007-238 and NSC 95-2120-M-007-012.

[1] H. Ennen, J. Schneider, G. Pomrenke, and A. Axmann, Appl. Phys. Lett. **43**, 943 (1983).
[2] G. Franzò, F. Priolo, S. Coffa, A. Polman, and A. Carnera, Appl. Phys. Lett. **64**, 2235 (1994).
[3] J. S. John, J. L. Coffer, Y. Chen, and R. F. Pinizzotto, J. Am. Chem. Soc. **121**, 1888 (1999).
[4] J. Wu, P. Punchaipetch, R. M. Wallace, and J. L. Coffer, Adv. Mater. (Weinheim, Ger.) **16**, 1444 (2004).
[5] Z. Wang and J. L. Coffer, Nano Lett. **2**, 1303 (2002).
[6] K. Suh, J. H. Shin, O. H. Park, B. S. Bae, J. C. Lee, and H. J. Choi, Appl. Phys. Lett. **86**, 053101 (2005).
[7] J. Wang, M. J. Zhou, S. K. Hark, Q. Li, D. Tang, M. W. Chu, and C. H. Chen, Appl. Phys. Lett. **89**, 221917 (2006).
[8] L. Zhao, T. Lu, M. Zacharias, J. Yu, J. Shen, H. Hofmeister, M. Steinhart, and U. Gösele, Adv. Mater. (Weinheim, Ger.) **18**, 363 (2006).
[9] J. H. Shin, M. J. Kim, S. Y. Seo, and C. Lee, Appl. Phys. Lett. **72**, 1092 (1998).
[10] M. Fujii, M. Yoshida, Y. Kanzawa, S. Hayashi, and K. Yamamoto, Appl. Phys. Lett. **71**, 1198 (1997).
[11] A. Polman, G. N. van den Hoven, J. S. Custer, J. H. Shin, R. Serna, and P. F. A. Alkemade, J. Appl. Phys. **77**, 1256 (1995).
[12] D. D. D. Ma, C. S. Lee, F. C. K. Au, S. Y. Tong, and S. T. Lee, Science **299**, 1874 (2003).
[13] Y. Huang, X. Duan, Y. Cui, L. J. Lauhon, K. H. Kim, and C. M. Lieber, Science **294**, 1313 (2001).
[14] Y. Cui and C. M. Lieber, Science **291**, 851 (2001).
[15] Y. Cui, X. Duan, J. Hu, and C. M. Lieber, J. Phys. Chem. B **104**, 5213 (2000).
[16] K. K. Lew, L. Pan, T. E. Bogart, S. M. Dilts, E. C. Dickey, J. M. Redwing, Y. Wang, M. Cabassi, T. S. Mayer, and S. W. Novak, Appl. Phys. Lett. **85**, 3101 (2004).
[17] W. S. Shi, H. Y. Peng, Y. F. Zheng, N. Wang, N. G. Shang, Z. W. Pan, C. S. Lee, and S. T. Lee, Adv. Mater. (Weinheim, Ger.) **12**, 1343 (2000).
[18] Q. Gu, H. Dang, J. Cao, J. Zhao, and S. Fan, Appl. Phys. Lett. **76**, 3020 (2000).
[19] R. Q. Zhang, Y. Lifshitz, and S. T. Lee, Adv. Mater. (Weinheim, Ger.) **15**, 635 (2003).
[20] V. Schmidt, S. Senz, and U. Göesele, Nano Lett. **5**, 931 (2005).
[21] M. Dovrat, N. Arad, X.-H. Zhang, S.-T. Lee, and A. Sa'ar, Phys. Rev. B **75**, 205343 (2007).
[22] S. M. Sze, *Physics of Semiconductor Devices*, 2nd edition (Wiley, New York, 1981), 304.
[23] J. L. Benton, J. Michel, L. C. Kimerling, D. C. Jacobson, Y. H. Xie, D. J. Eaglesham, E. A. Fitzgerald, and J. M. Poate, J. Appl. Phys. **70**, 2667 (1991).
[24] Y. L. Chueh, L. J. Chou, S. L. Cheng, J. H. He, W. W. Wu, and L. J. Chen, Appl. Phys. Lett. **86**, 133112 (2005).
[25] Y. H. Tang, X. H. Sun, F. C. K. Au, L. S. Liao, H. Y. Peng, C. S. Lee, S. T. Lee, and T. K. Sham, Appl. Phys. Lett. **79**, 1673 (2001).
[26] H. W. Wu, C. J. Tsai, and L. J. Chen, Appl. Phys. Lett. **90**, 043121 (2007).